Materials and Structures (2016) 49:1337–1350
DOI 10.1617/s11527-015-0580-z

ORIGINAL ARTICLE

An anchoring element for prestressed FRP reinforcement: simplified design of the anchoring area

František Girgle · Petr Štěpánek

Received: 1 October 2014 / Accepted: 2 March 2015 / Published online: 7 March 2015

Abstract Today, fibre-reinforced polymers (FRP) are widely used construction materials. The use of non-metallic reinforcement as inner reinforcement has many advantages, as is well known, but there are some areas of application that need to be resolved in order to improve the usage of FRP reinforcement in real-world conditions. One of these is the design of a suitable anchorage for prestressed FRP applications. It is difficult to design a safe anchorage using conventional methods of anchoring (systems for the anchorage of steel tendons) due to the well-known low compressive strength perpendicular to the fibres, this being due to the anisotropy of composite materials. Most of the anchoring systems commonly used worldwide are based on the use of metal parts (steel tubes, wedges, etc.) in a system which is primarily designed to be non-metallic. It is in contradiction with the initial intention to use non-metallic reinforcement. The presented text describes the basic physical and mechanical properties of a developed non-metallic anchor element. The essential principles of an analytical solution of the developed anchoring element based on the stiffness parameters of the system's individual components are also presented. The behaviour of each material used is described in terms of simplify form. The functionality of the anchoring system was verified by a number of load tests and the obtained results were compared with theoretically and numerically calculated values. The presented results show the high efficiency of the anchoring system as well as the suitability of the derived analytical solution for simplified design and evaluation of the anchoring area.

Keywords FRP reinforcement · Non-metallic · Anchorage · Analytical solution · Pull-out

F. Girgle (✉) · P. Štěpánek
Faculty of Civil Engineering, Brno University of Technology, Brno, Czech Republic
e-mail: girgle.f@fce.vutbr.cz
URL: http://www.fce.vutbr.cz

P. Štěpánek
e-mail: stepanek.p@fce.vutbr.cz
URL: http://www.fce.vutbr.cz

1 Introduction

Fibre-reinforced polymers (FRP) used as inner reinforcement in concrete members are, especially in the case of members exposed to demanding environmental conditions, regarded as a better alternative to steel bars due to their resistance to corrosion, their nonmagnetic behaviour, and also their very good strength to weight ratio. One of the disadvantages of FRP reinforcement is its lower modulus of elasticity (especially in the case of commonly-used GFRP reinforcement). This leads to lower stiffness and thus to greater deflections of structures, and can also cause early propagation of cracks (see e.g. [17]). The paper deals with the possibility of eliminating this problem

by prestressing the reinforcement. It is especially focused on the description of the behaviour of the anchoring area of the own developed anchoring element, which is based on the creation of an additional spreading area in the anchorage zone of (not only) prestressed reinforcement by casting.

It is difficult to design a safe anchorage due to the anisotropy of composite materials and their low compressive strength perpendicular to the fibres. While using standard anchoring cones with jagged surfaces the following forces arise in prestressed reinforcement– axial tension, longitudinal shear and transverse compression. Erki and Rizkalla [7, 8] introduced basic types of anchorages for commonly used types of tendons which can be divided into two main groups-mechanically based anchors ("wedge type anchor") and bond based anchors ("grout type anchor"). A considerable number of anchoring systems have been developed or modified during the last few decades (see e.g. [6] or [10]). Unfortunately, most of them rely on steel parts (e.g. [1, 2, 8, 13, 16, 21, 22]), which is in contradiction with the initial intention to use non-metallic reinforcement and to take advantage of its lack of corrosion risks or use its other positive aspects. This was the main reason for the development of a grout-based anchoring system which does not rely on any metal parts (see [9 or 18]).

Although a lot of experimental work has been carried out on grouted FRP bars anchored in steel tubes filled with epoxy resin or mortar, theoretical studies regarding the prediction of anchor tensile capacity are relatively a few in the literature. They primarily consist of the seminal work by Zhang et al. [20] and newer works mostly based on Zhang (e.g. 12, 14, 15, 19]). Most of these works are dedicated to systems based on the use of steel tubes as the basic part of the anchor, and cannot be used in general conditions. Furthermore, the derived formulas are often accurate but too complicated for common use.

For the above-mentioned reasons, the theoretical part of the development of the anchoring system was aimed at the derivation of simplified forms of equations that are easy to use in design practice. A description of the theoretical behaviour of an anchoring area is presented in the paper. The behaviour of the anchoring area is described by using the stiffness parameters of its individual components. Finally, a comparison of data obtained from numerical and analytical calculations with data obtained from experiments is presented.

2 The developed anchor element

Between 2008 and 2009, a system of anchoring prestressed FRP reinforcement (published for example in [9 or 18]) was developed during research and development activities conducted at the Faculty of Civil Engineering at Brno University of Technology. The anchoring system is based on the creation of an additional spreading area in the anchorage zone of prestressed reinforcement. This area allows the efficient transfer of prestressing force into the surrounding concrete (idealized shape is depicted in Fig. 1). Thus, the anchoring length is significantly shorter than the normal necessary bonded length of straight tendon. The area is created by attaching one or more anchoring rollers manufactured from a special polymer compound (made up of a special mixture) with a larger diameter than the diameter of the reinforcement (see Fig. 2). The diameters, lengths and also number of rollers are variable. See the figure below (Fig. 1) for an idealized working diagram of the anchor element. In the figure, F denotes the anchored force, L_k the length and D_k the diameter of the anchoring element. The colours used depict the type of acting forces-red for compression, green for tensile forces acting on the end of the anchor and blue for the shear forces on the surface of the anchor. The behaviour of the anchor will be described in more detail in Chap. 3.

Anchoring elements can be optionally arranged in series, either to increase the loading capacity and safety of the anchorage system or to reduce the deformation in the anchorage area (the anchorage area is stiffer).

Anchors are made from a special thermosetting polymer compound with mineral fillers (reinforcing fibres may be used to increase the tensile strength) which is injected into a removable form and thereafter hardened. The material of the anchor has excellent cohesion with the reinforcement and due to this it is possible to transfer tensile force via a shorter anchorage length. The anchoring element is simple to implement, both in the preparation as well as their subsequent implementation. The anchors are intended mainly for precast elements but can be used also for additionally prestressed members. In addition, the

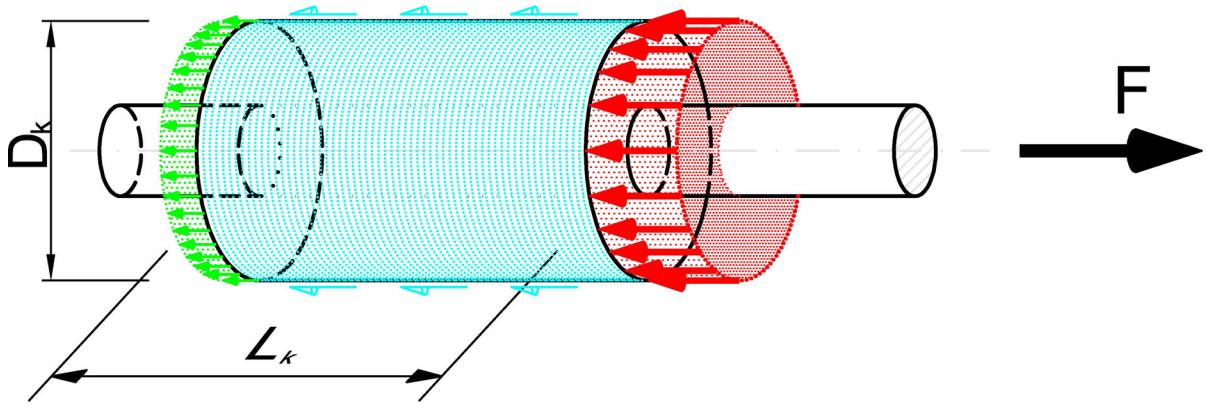

Fig. 1 The developed anchoring element—an idealization of forces acting on one anchor (*red*-compression, *green*-tensile, *blue*-shear)

Fig. 2 Anchoring element cut horizontally

developed anchoring system offers all the advantages of using FRP reinforcement.

3 Analytical solution of the anchoring area

The goal of the presented analytical solution is to describe the dependence of the anchored force on the slip of the embedded prestressed reinforcement, and also to quantify the prestressing loss due to the slip in the reinforcement/anchor and anchor/concrete interface. The main transfer of anchored force into the surrounding concrete takes place in the heads of anchors. Anchors create "stops" in the concrete and can be idealized as springs pressing against the concrete in the heads of anchors. It is therefore convenient to describe the behaviour of the anchoring area by using the stiffness parameters of its individual components (as opposed to the approach used in the above-mentioned works based on Zhang [20]). The derived equations describe the dependence of prestressing force on the deformation (slip) of particular parts of the anchoring area. Furthermore, the modification of the anchoring area (addition of another anchoring element, etc.) is possible without any expressive redesign of the given solution.

3.1 Basic assumptions

The following assumptions are held for the presented analytical solution:

(a) The material of the anchoring element (grout anchor) will behave in an elastic manner until the failure;
(b) The behaviour of the surrounding concrete and FRP reinforcement is fully described by the constitutive law;
(c) The anchored force is distributed from the reinforcement into the anchor via shear forces acting on the interface between the anchor and the reinforcement in accordance with the defined constitutive law (hence, the interface is considered to be a particular material in the presented solution);

(d) The cooperation between the reinforcement and the anchoring element takes place along the whole length of the interface;
(e) The stresses on the cross-section (anchor, reinforcement) are distributed uniformly;
(f) The behaviour of the anchor is considered rigid when calculating the strain of the surrounding concrete below the head of the anchor;
(g) The diameter of the anchored tendon is considered constant along the entire length of its anchoring area.

The anchoring system can be idealized, in accordance with the above-mentioned assumptions, as a system of springs arranged in series (see Fig. 3) together accounting for the transfer of the anchored force to the surrounding concrete.

In the aforementioned figure, L denotes the length of the whole anchoring system, L_k^j the length and D_k^j the diameter of the *j-th* anchoring element, and S_v^j the distance between anchoring elements j and $j+1$ (or the depth of the spreading area, which is affected by the distance between the anchor and an edge of the concrete member, and by the spacing of the anchoring elements). E_k^j and A_k^j are Young's modulus of elasticity and the cross-section area of the *j-th* anchoring element, respectively, E_v and A_v represent Young's modulus of elasticity and the cross-section area of the anchored FRP reinforcement of diameter d_v ($d_v < D_k^j$), respectively, and F is the anchored prestressing force.

The anchored force consecutively activates each of the springs, which bears a force proportional to its actual stiffness. The total bearing capacity is given as a sum of the forces from the pressed surface areas (heads) of the anchors and the forces arising from shear between the anchor surface and the surrounding concrete and friction between the reinforcement and the surrounding concrete (see Fig. 1).

The whole anchoring system is composed from (see Fig. 3):

(a) The reinforcement in front of the 1st anchor (given A_v and E_v);
(b) The surrounding concrete (given: material characteristics, especially modulus of elasticity E_c and compressive strength f_{ck});
(c) N_k anchoring elements (given: A_k, E_k and the length of anchor L_{ki}), where N is the number of the anchoring elements;
(d) N_k–1 reinforcements between the anchoring elements (given: A_v, E_v, the length of reinforcement between the anchoring elements S_{vi}).

Each *j-th* anchoring element can be divided into n_i segments with segment length $l_{k,i}$, and each *j-th* reinforcement between the anchoring elements can be divided into m_i segments with segment length $s_{v,i}$ (see Fig. 4) in such a way that:

$$\sum_{j=1}^{N} L_k^j + \sum_{j=1}^{N-1} S_v^j = L, \tag{1}$$

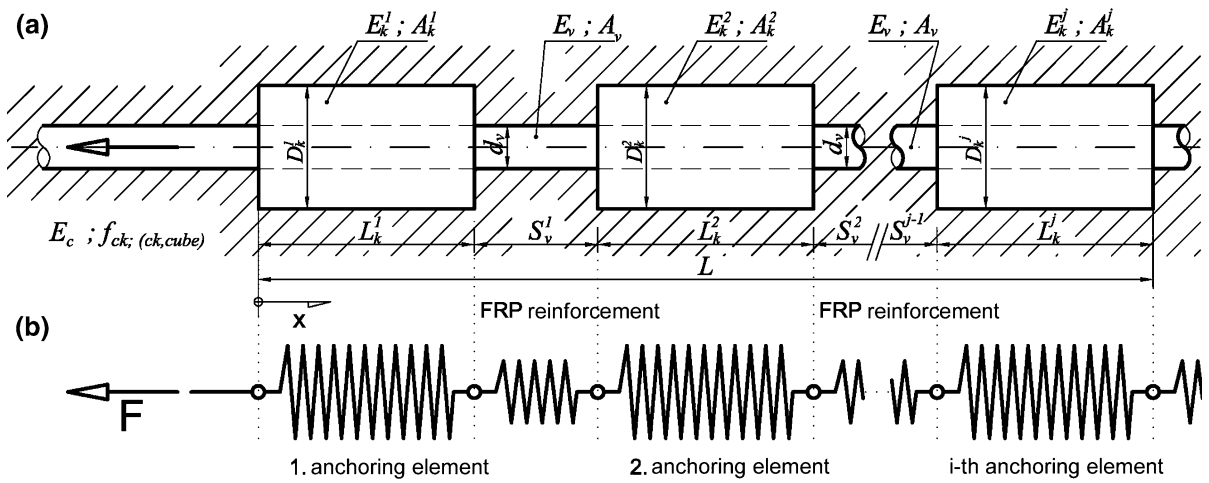

Fig. 3 The anchoring area **a** real shape; **b** idealized behaviour

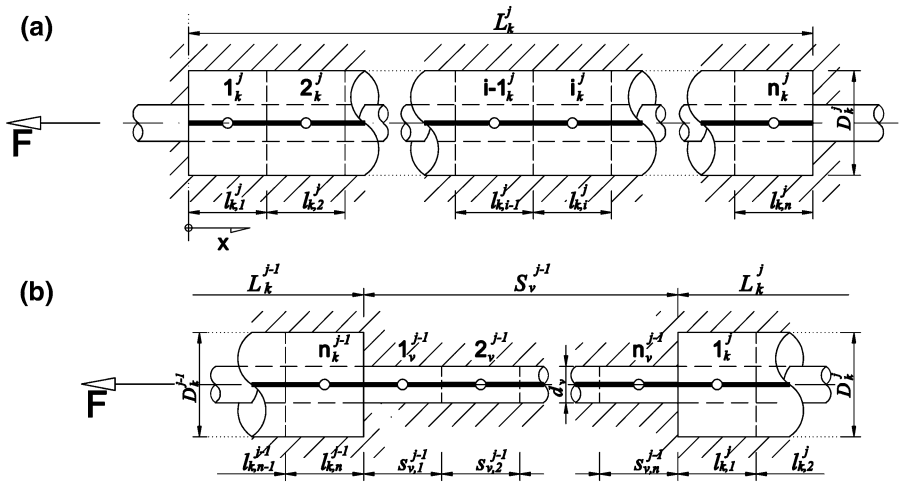

Fig. 4 The principle behind the splitting of the anchorage area into individual elements; **a** anchoring element, **b** tendon between anchors

$$\sum_{i=1}^{n} l_{k,i}^{j} = L_k^j, \tag{2}$$

$$\sum_{i=1}^{\overline{m}} s_{v,i}^{j} = S_v^j, \tag{3}$$

where $l_{k,i}^{j}$ is the length of the *i-th* element from the *j-th* anchoring element and $s_{v,i}^{j}$ is the length of the *i-th* element from the *j-th* reinforcement between the anchoring elements.

Each of the sub-elements (segments) of the anchoring system (see Fig. 4) can be idealized by a single reference point located in the centroid of the segment (i.e. for a rod segment of constant cross-section in the middle of its length) and its corresponding unknown displacement. Based on the known stiffness parameters of the system segments (i.e. knowledge of E_v, E_k, A_v and A_k), and by using elementary elasticity equations, the deformation state can be calculated at each reference point of the anchoring system.

For each system reference point (based on the constitutive law describing the behaviour of the interface) it is possible to determine the bond stress-strain dependence; in other words, to calculate the particular force F_i^j according to the following Eq. (4):

$$F_i^j = \tau\left(u_i^j\right) \cdot l_{k,i}^{j} \cdot \pi \cdot d_v, \tag{4}$$

where $\tau(\, u_i^j)$ is the bond stress between the reinforcement and the anchoring element of the *i-th* element of the *j-th* anchor (for the constitutive law describing the behaviour of the interface see Chap. 3.3.1) and u_i^j is the slip of the reinforcement in the interface between the reinforcement and the anchoring element of the *i-th* elements of the *j-th* anchor.

The resulting loading capacity of the anchoring system is given as the sum of the resistances of its segments, i.e. the sum of the contributions of anchoring elements and reinforcements between the anchoring elements according to the following equation:

$$\sum_{i=1}^{N}\sum_{j=1}^{n} F_{k,i}^{j} + \sum_{i=1}^{N-1}\sum_{j=1}^{\overline{n}} F_{v,i}^{j} = F. \tag{5}$$

In the above-mentioned equation, $F_{k,i}^{j}$ denotes the resistance of the *j-th* segment of the *i-th* anchoring element, and $F_{v,I}^{j}$ is the resistance of the *j-th* segment of the *i-th* reinforcement between anchoring elements, N represents the number of anchoring elements in the anchoring system, and n (or $\overline{n}$) is the number of sub-segments of each anchoring element in the system (or reinforcement between anchoring elements).

A basic deformation equation for the general *i-th* reference point of the anchoring system can be expressed as follows [Eq. (6), see Fig. 5]:

$$u_{i-1} + u_{k,i-1} + u_{c,i-1} = u_i + u_{k,i} + u_{v,i} + u_{c,i}, \tag{6}$$

where u_{i-1} and u_i are the slips in the interface between reinforcement and anchor at the $i-1$ and *i-th* reference point, respectively, $u_{k,i-1}$ and $u_{k,i}$ are the slips caused by elastic deformation of the anchor at the $i-1$ and *i-th* reference point, respectively, $u_{c,i-1}$ and $u_{c,i}$ are the slips caused by deformation of concrete in the anchor

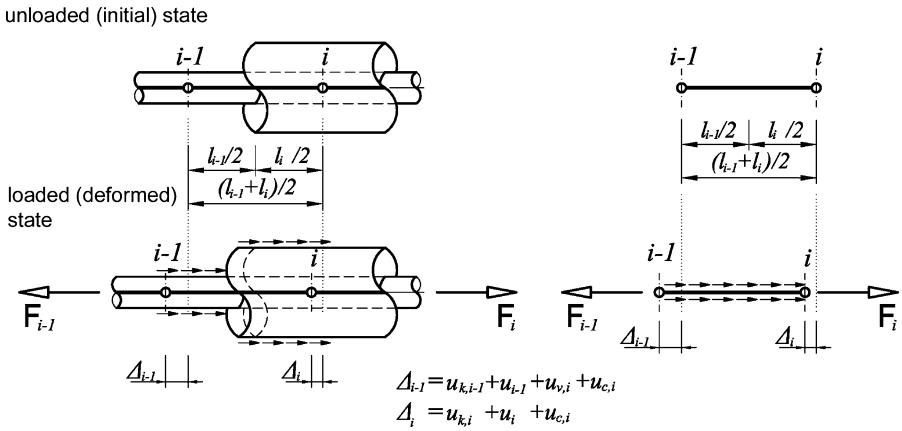

Fig. 5 Anchoring area–deformation behaviour of the anchor element

head, and $u_{v,i}$ is the slip caused by elastic deformation of the reinforcement between the solved points-it is assumed that this elastic deformation is caused by force transmitted by the previous sub-segment (i.e. the reference point of segment *i*-1).

The basic deformation Eq. (6) is subsequently modified according to the position of solved nodes in the anchoring system:

(a) The equation for the first reference point of the anchoring element must take into account the deformation of concrete in the head of the anchor caused by the transmission of force from the anchor to the surrounding concrete; and also the deformation of the anchor between the head and the first node, which activates friction on the surface;
(b) The equation for the first to *n-th* reference point of the anchoring element reflects the deformation of the anchor, which activates friction on the surface;
(c) The equation for the last reference point of the anchoring element takes into account the deformation of the anchor between the last node and the end of the anchor, via which friction on the surface is generated. It is also possible to include the tension between the end of the anchor and the surrounding concrete in the equation (see Fig. 1), but this is obviously insignificant;
(d) The equation for the general reference point (i.e. the first to *n-th*) of the reinforcement between anchoring elements reflects the deformation of the reinforcement and thus also the friction which is generated on the surface of the reinforcement.

3.2 Calculation method

For each part of the anchoring system (N anchoring elements and $N-1$ reinforcements between the anchors) with n individual segments, exactly n equations of continuity (6) are assembled (for $n+1$ unknown slips, including the starting slip in the head of the anchor) and modified depending on the position of the solved nodes in the anchoring system. They are then included in the global matrix via the position of their reference points in the system.

The unknown values of deformations for one anchoring element divided according to Eq. (2) into n sub-segments can be calculated (by using Eq. (6) and elementary elasticity equations describing the stiffness of the springs) in the following manner:

– *The slip in the interface* u_i is always caused by the particular appertained force. Thus, it is always the unknown parameter of calculation and can be written for the whole anchor as a column vector of slips $\mathbf{u_{(n+1,1)}}$ about $n+1$ unknowns. The slip in the anchor head u_0 (starting slip) is generally nonzero;
– *The slip of the reference point* $u_{k,i}$ caused by the elastic deformation of the anchor is established with an assumption of the particular forces (obtained from sub-elements of the split anchor) acting on the appropriate length of anchor. This system of equations, assembled for the whole anchor, can be written in matrix form as follows;

$$\mathbf{u_k} = \mathbf{K_{k(n,n)}}\,\mathbf{f_{(n,1)}}, \tag{7}$$

where $\mathbf{K_{k(n,n)}}$ is the symmetrical square matrix of the anchor's stiffness. The type of matrix is (n,n),

where n is equal to the number of sub-elements. $\mathbf{f_{(n,1)}}$ is the column vector of acting forces $\overline{F_i}$ calculated for each node 1 to n. The resulting value of the nodes' slips caused by the deformation of the anchor is the column vector $\mathbf{u_k}$ of n rows.

– *The slip of the reference point* $u_{v,i}$ caused by the deformation of the FRP reinforcement is established with the assumption that a force from a given sub-element is acting on an active length of the reinforcement (i.e. on the length of the reinforcement where the force has an effect and causes the deformation). The following equation for n sub-elements must be valid:

$$\mathbf{u_v} = \mathbf{f_{(n,1)}}\,\mathbf{k_{v(1,n)}}, \tag{8}$$

where $\mathbf{f_{(n,1)}}$ is the column vector of forces acting on an appropriate active length and $\mathbf{k_{v(1,n)}}$ is the vector of the reinforcement's stiffness constants. The resulting value of the nodes' slip caused by the deformation of reinforcement is the column vector $\mathbf{u_v}$ of type (n,1).

– *The slip of the reference point caused by the deformation of the concrete in the head of anchor* u_c is established with the assumption that the sum of all particular forces F_i (see Eq. (4)) of the given anchor acts on the stiffness springs substituting for the surrounding concrete in the head. If only one anchoring element is taken into account then the value u_c will be the same for all calculated deformation Eqs. (6). The value u_c for the last node of the previous and the first node of the next anchor will generally be different only in the case of anchoring systems with more than one anchor. The value of concrete deformation in the head of an anchor can be calculated by the following equation:

$$u_c = \alpha \cdot \frac{\sum_{i=1}^{n} F_i}{K_c}, \tag{9}$$

where K_c is the actual stiffness of the surrounding concrete in the head of the anchor and ΣF_i is the sum of all particular forces acting on the given anchor. The stiffness K_c can have two limit values depending on the level of stresses in the concrete below the anchor's head—i.e. if the concrete exhibits elastic or plastic behaviour.

The coefficient α takes into account the influence of the edge condition on the deformation of concrete. The coefficient α is equal to 1.0 for an element anchored in the continuum (i.e. without the influence of the edge of the concrete member); for the case with the influence of the edge α is always >1,0. The method for determining the coefficient α is presented in Chap. 3.4.

For each part of the anchoring system (N anchoring element and N-1 reinforcement between anchors) with n individual segments, exactly n equations of continuity (6) are assembled and modified depending on the position of the solved nodes in the anchoring system. They are then included in the global matrix via the position of their reference points in the system. Therefore, the unknown slips u_0 to u_n, stiffness and length constants (E, A, l) and forces F_1 to F_n can be found in the matrix. The mentioned forces can also be written (see Eq. (4)) as a function of variable u.

The above-mentioned system of n linear equations with $n + 1$ unknowns can be solved by known mathematical solution methods. However, depiction of the dependence between the anchored prestressing force and the slip in the head of an anchor (via a so-called "working diagram") is very useful for designing the anchoring area and can be obtained from the solution. By substituting an unknown deformation parameter for a specific value (for the determination of a "working diagram" it is appropriate to select a value of deformation at the zero point u_0) there will be exactly n unknown values in the matrix of linear algebraic equations with n lines.

This system of linear equations with the same number of equations as unknown values can already be easily solved. The deformation state (i.e. the slip in each node of the system) of the anchor area is obtained from the suggested analytical solution. The total force F from each of the deformation states of the anchoring area (i.e. for each of the pre-described slips u_0) can be calculated now. When the slip in the zero node is selected repetitively and the system is resolved, particular points of slip-force dependence will be obtained. The "working diagram" of the anchoring area is defined by a line connecting these points.

The suggested analytical solution, if it is used in its full form, can lead to a considerably large system of equations and, therefore, is primarily intended for the automation of their solution utilising software tools. Simplification of the calculation can be carried out in a number of ways which have a different effect on the accuracy of the final solution. It is always necessary to

choose a method of calculation which is able to predict real behaviour with the sufficient accuracy.

3.3 Determination of the stiffness parameters of individual components

It is necessary to determine the stiffness parameters of each of the individual components of the anchoring system before drawing up the global matrix—i.e. the surrounding concrete, the anchoring elements, the reinforcement and the interface between the anchored reinforcement and the anchoring element. The calculation of the stiffness parameters of the surrounding concrete and the interface will be briefly shown in the following text. The stiffness parameter calculations for the reinforcement and anchor are based on well-known basic elasticity equations and their subsequent implementation, and thus will not be shown.

3.3.1 The interface between the reinforcement and anchoring element

The constitutive law describing the behaviour of the interface between the anchored reinforcement and the anchoring element (i.e. the dependence of bond stress on the slip in the interface; the bond-slip model—see e.g. [23]) is strongly subject to the type of anchored reinforcement (modulus of elasticity, type of coating, etc.) and the material from which the anchors are made. The presented equations describing the interface behaviour are based on data obtained from the experimental part of the development of the anchor. All tested types of anchors have brittle behaviour (see Fig. 6). The constitutive law is usually composed of two branches. The first increasing branch (a linear, bi-linear or nonlinear relationship can be assumed); the second branch describes the softening behaviour of the interface after reaching the peak of bond stress, and it can be assumed to be linear.

According to the data obtained from experiments, only the linear relationship in the increasing branch is sufficient to accurately describe the interface behaviour for anchoring elements shorter than 70 mm (see Fig. 6). It is convenient to use the bi-linear path in the increasing branch for greater anchoring lengths.

The performed experimental tests indicate the direct dependence of the derived constitutive law on the length of the anchoring element. Longer anchors show a lower stiffness than shorter ones, i.e. for the same slip a higher bond stress value is reached for shorter anchors than for longer anchors (see Fig. 6). The failure of anchors shorter than 30 mm occurs suddenly without visible deformation. For the dependence of the interface stiffness on the length of the anchor element and also on the level of anchored force see Fig. 7.

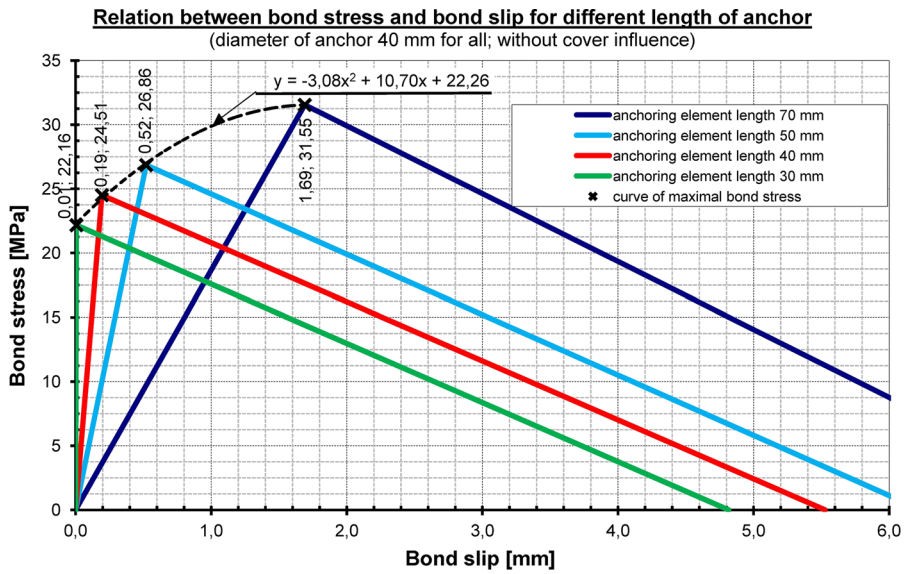

Fig. 6 The dependence of the bond stress and bond slip for different anchor *lengths* (for all *lengths* $D_k = 40$ mm, with no influence from the element's edge)

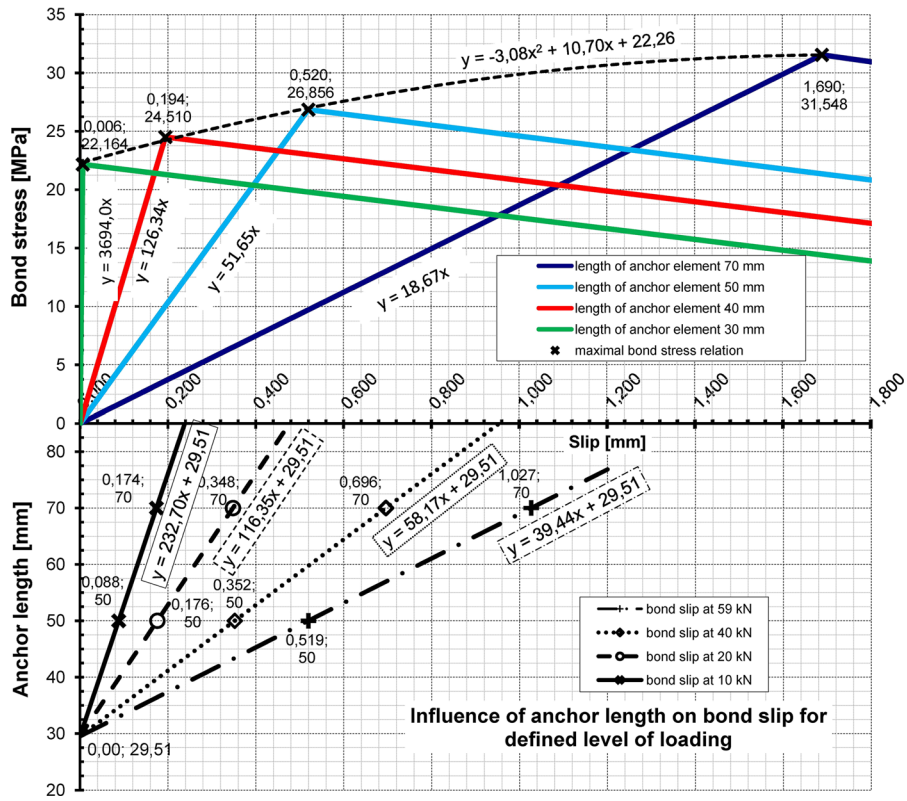

Fig. 7 The relation between the bond stress, the bond slip and also the influence of anchor length; the values are valid for anchors not influenced by the element's edge

3.3.2 The surrounding concrete

The approach used for determining the concrete stiffness in the anchor's head is based on the description of the interaction of the anchor head with the surrounding concrete, which is simplified via the effect of springs added directly below the anchor's head and the effect of shear spreading to the surroundings of the anchor's head (a modification of Pasternak's subsoil principle [11]).

Concrete behaviour is described by the bilinear constitutive law (according to [5]), which is used to calculate the stiffness parameters of the surrounding concrete.

The stiffness of concrete in the head of anchor $K_{c,i}$ is derived as the sum of the stiffness of concrete directly in the head of anchor $K_{c,i}^{w}$ (which is considered to have a constant value over the entire area) and the contribution of the surrounding concrete in the effective area of shear spreading $K_{c,i}^{P}$, which is considered as a spring acting on the circumference of the anchor head (see Fig. 8).

Figure 8 shows the assumed behaviour of the surrounding concrete in the case of the first anchor (or if $S_v > 2D_k$; see Fig. 8a) and also in the case if the distance between the anchors is lower than $2D_k$ ($S_v < 2D_k$; see Fig. 8b). The presented limit value of distance $2D_k$ is derived from the performed numerical simulations of the behaviour of the surrounding concrete. The deformation of the surrounding concrete caused by shear spreading is insignificant after the above-mentioned distance.

The deformation curve describing the shear spreading can be written (based on the equations presented in [11]) using the following equations (the origin of the coordinate is assumed to be in the centroid of the anchor's head):

$$u_{c,i}(x) = u_{c,i}^{0} \cdot e^{-\frac{x-D/2}{S}}, \tag{10}$$

where S is the constant of damping, which must be derived for each different combination of concrete class and anchor diameter, $u_{c,i}^{0}$ the deformation at the beginning of the shear spreading deformation curve,

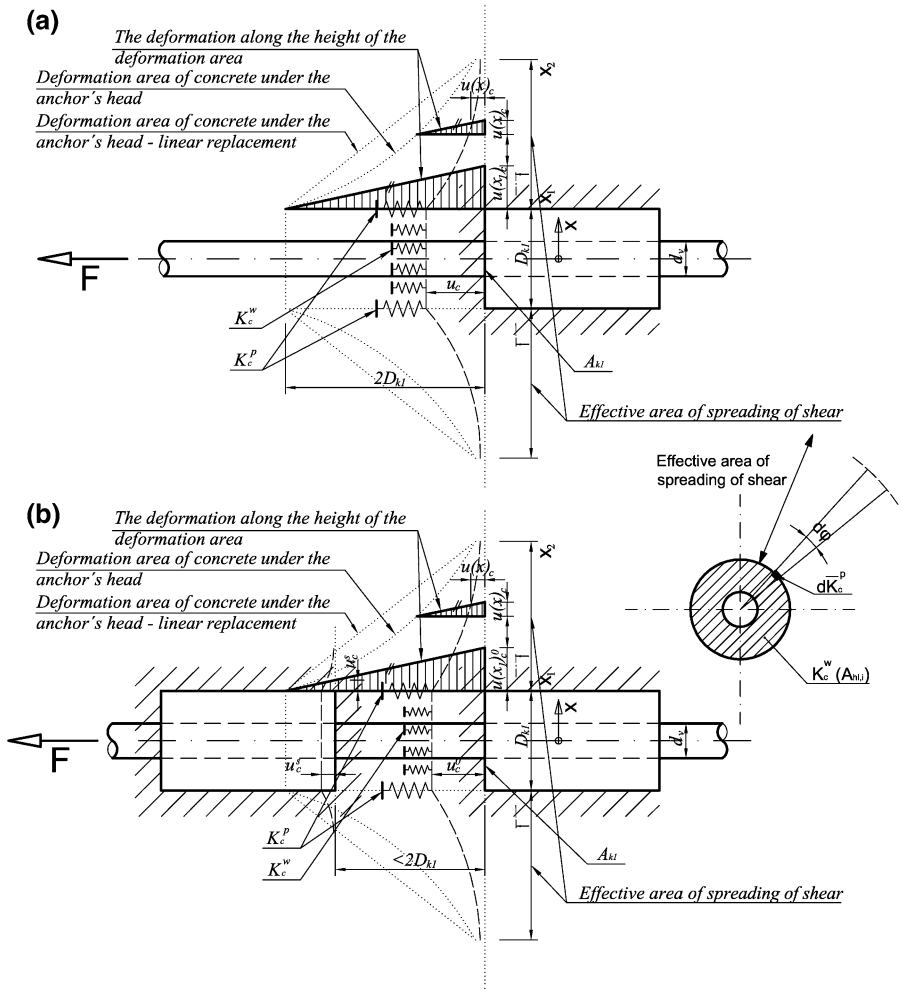

Fig. 8 Idealization of the behaviour of concrete under the anchor's head

and x the distance of the coordinate from the beginning of the coordinate system.

For the calculation of the stiffness parameters of the surrounding concrete $K^P_{c,i}$ the integration of Eq. (10) must be performed. The following Eq. (11) is derived for the case of an anchor acting uninfluenced by the member's edge (integration of the Eq. (10) at interval $<0; 2\pi>$); also, the depth of the deformation area H_i below the anchor's head is assumed to be constant.

$$K^P_{c,i} = \pi \cdot D_{k,i} \cdot \frac{E(\varepsilon_c)}{H_i} \cdot S \cdot \left[-e^{\frac{D_{k,i}-2x}{2S}}\right]_{x1}^{x2} = \pi \cdot D_{k,i} \cdot \frac{E(\varepsilon_c)}{H_i} \cdot S \cdot \left(-e^{\frac{D_{k,i}-2x_2}{2S}} + 1\right). \quad (11)$$

The stiffness of the concrete in the head of anchor $K^w_{c,I}$ can be calculated using this well-known equation

$$K^w_{c,i} = \frac{E(\varepsilon_c) \cdot A_{k,i}}{s_i}, \quad (12)$$

which is usable for the first anchor element or if the distance between the anchors s_i is greater than or equal to $2D_k$. In case of $s_i < 2D_k$ is necessary to modify the above-mentioned Eq. (12) into the following form:

$$K^w_{c,i} = \frac{E(\varepsilon_c) \cdot A_{k,i}}{2D_{k,i}} \cdot \left(1 - \frac{2D_{k,i} - s_i}{2D_{k,i}}\right). \quad (13)$$

3.4 Solution of an anchoring area influenced by a concrete member's edge

If the anchoring area is placed near to the edge of a concrete member, it is clear that the calculation cannot be performed with all of the assumptions valid for an

anchoring system placed in a continuum of concrete without the influence of cover, and must be modified. However, it is only possible to modify the constitutive relationship describing the behaviour of concrete. Thus, the influence of the edge can be taken into account by calculating the different stiffness by modifying the limits of integration according to Eq. (10). These stiffness parameters are consequently inserted into the calculation, which is not different from the previous one.

The part of an anchoring area close to the member's edge does not allow the full dissipation of the deformation below the head of the solved anchor. Therefore, the calculated values of the stiffness parameters $K_{c,i}^{P}$ close to the edge will be lower (see Fig. 9; $K_{c,i}^{P1}$ and $K_{c,i}^{P2}$ below and above the solved anchor axis; $K_{c,i}^{P2} < K_{c,i}^{P1}$).

Due to the assumption of the uniform distribution of the stress directly below the anchor's head it is clear that the centroid of the stiffness spring system is shifted from the axis of the anchored reinforcement (eccentricity r is created). Therefore, the anchoring area is loaded by the combination of normal force and moment action. The acting moment increases the deformation of concrete in the head of anchor u_c and also reduces the bearing capacity of the anchoring system. Therefore, it is necessary to include coefficient α [see Eq. (9)], which takes the influence of the edge into account.

The coefficient α can be written in the form:

$$\alpha = 1 + k \cdot \frac{r \cdot u}{W}, \tag{14}$$

where r is the eccentricity caused by different stiffness parameters, u the perimeter of the critical section where the moment is acting, W the plastic section modulus of the critical section, and k the influence of shear in the critical section. The value of coefficient k must be obtained from experiments ($k \leq 1.0$; in the absence of the exact values it can be considered equal to 1.0).

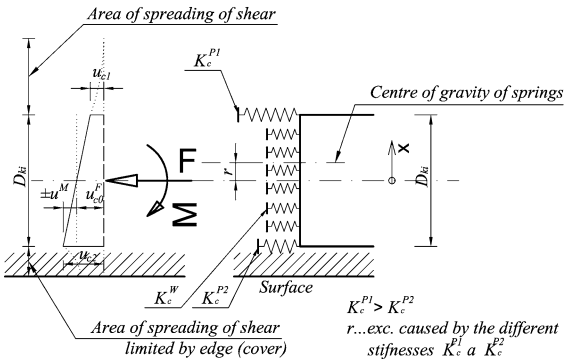

Fig. 9 The influence of the different stiffnesses of the springs

4 Solution results

The functionality of the anchoring system for prestressing reinforcement has been verified through a series of pull-out tests. Different anchoring element lengths were tested–anchor lengths of 40, 50 and 70 mm were tested as a "single anchor element", and an anchoring element with a length of 30 mm was tested in series (two elements in the anchoring area). 14 mm diameter GFRP bars and surrounding concrete of type C30/37 were used for all tested configurations of the anchoring area. The experiments carried out on anchoring elements showed the high efficiency of the system. The configuration of the pull-out tests and also the parameters of materials were presented in full in previous papers (see e.g. [18]) and it will not be mentioned in this paper. However, the results obtained from pull-out tests are used for comparison with the results from analytical solution.

As an inseparable part of the development and consequent verification of the anchor, numerical simulations of the anchoring area were also performed. Numerical simulations were carried out in ATENA FEM software (Červenka Consulting; [3, 4]).

The results obtained from the above-mentioned analytical and numerical solution are displayed in the form of a "working diagram" (depicting the relation between the applied force and bond slip) of the anchoring area. It is very useful for anchoring area design, as it enables the design of an anchoring area both in terms of determining the maximum loading capacity and also in terms of the calculation of the slip caused by the applied force.

An example of an evaluation of the obtained results is shown in Figs. 10, 11. Figure 10 compares the load curve gained from nonlinear calculations in ATENA software with a "working diagram" of the anchoring area obtained from the solution of derived analytical equations (for the number of reference points on the anchor n = 3) and also data from load tests performed on real specimens. Their anchoring areas are each

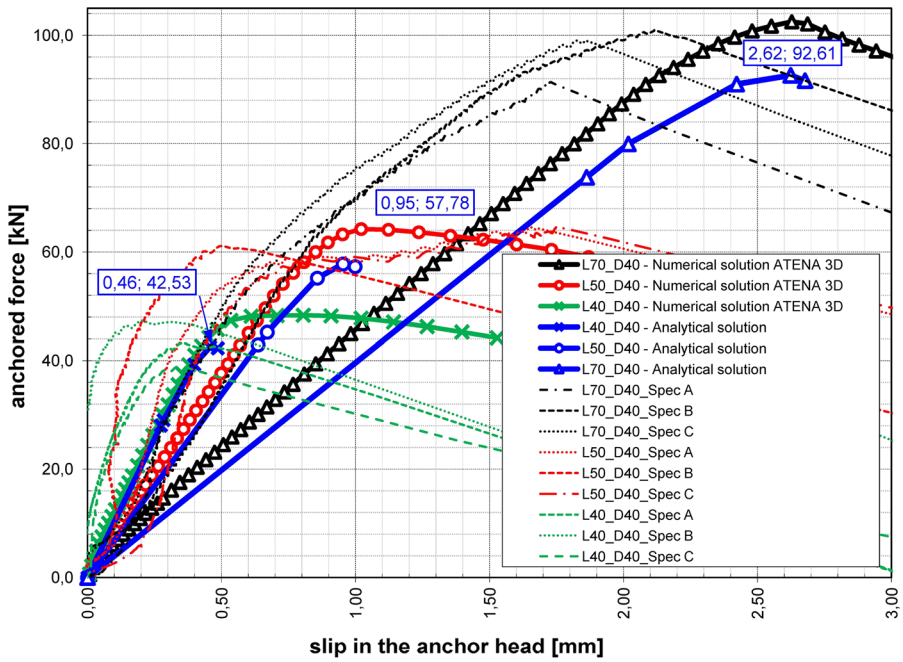

Fig. 10 Comparison of results obtained from experiments, numerical and analytical solutions for anchoring elements without edge influence

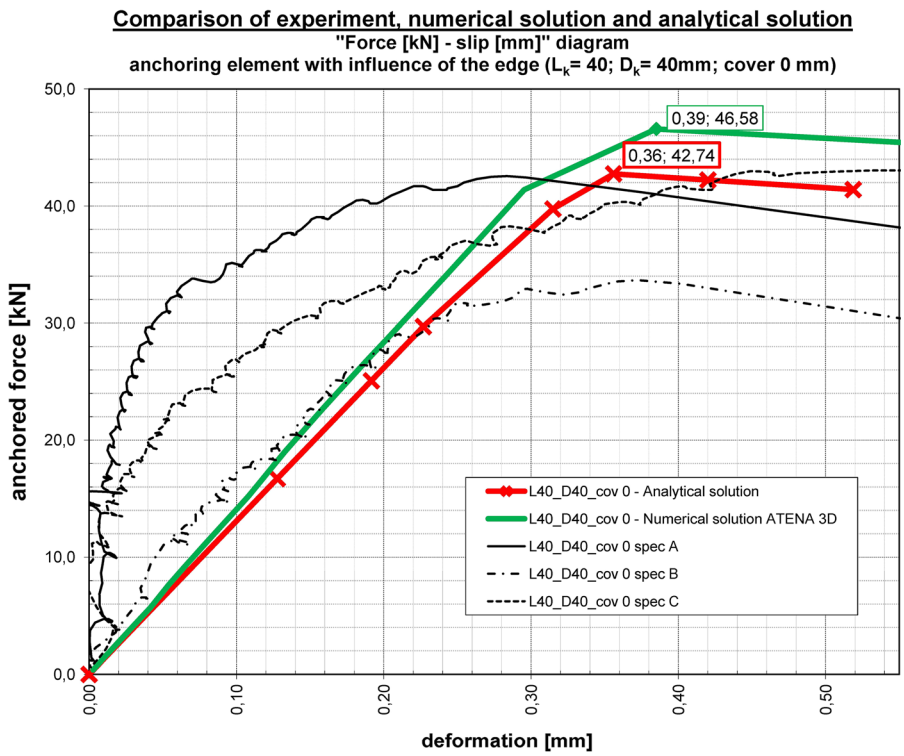

Fig. 11 Comparison of results obtained from experiments, numerical and analytical solutions for anchoring elements with edge influence (*cover thickness* 0 mm)

implemented using a single anchoring element with a length of 70, 50, or 40 mm without the influence of the member's edge.

Figure 11 shows the results obtained from the analytical and numerical solution and also load testing data for an anchoring element with edge influence.

The anchor element is 40 mm long with a diameter of 40 mm and a cover thickness of 0 mm.

Significant scatter of results can be observed especially for specimens with influence of edge (see Fig. 11, black lines). It has been caused mainly by the manner in which specimen fails. The failure of specimens with influence of edge, which exhibit considerable dispersion of the obtained values, occurs by splitting of concrete cover.

There is good correlation between the analytical solutions and the numerical model in determining the maximum force imposed at the failure of the anchoring area. Moreover, better fitting values are provided by the analytical solutions than by the numerical calculation (see Fig. 10). When calculating the slip in the anchor head, however, the analytical model (and also the numerical solutions in ATENA FEM software) has lower stiffness (gives higher values of slip) compared to the experiment—it is evident from Figs. 10, 11. This is caused by the given assumptions of the numerical and analytical calculations. The cohesion between anchor's surface and surrounding concrete and also the cohesion between the end of anchor and concrete has been neglected. These assumptions have been taken into account for both of these. This is the main reason for softer behaviour of calculated curves in comparison with the test results.

5 Conclusion

Derived analytical equations can predict with a high degree of accuracy the behaviour of an anchoring area with or without the influence of boundary conditions mainly in terms of bearing capacity. However, they are very sensitive to input constitutive equations describing the behaviour of implicated materials. It is therefore necessary to standardize mainly the raw materials and manufacturing techniques used to produce anchoring elements, as they have a significant impact on the behaviour of the interface between the anchoring element and the anchored reinforcement. The calculation method described in the article gives conservative results. It provides almost the same level of bearing capacity as results obtained from experiments, but with a higher degree of deformation (i.e. lower anchoring area stiffness).

The theory described in the article can (with the application of appropriate constitutive equations describing the behaviour of basic materials) be used for the design of elements from all known types of FRP reinforcement, and it is not limited by the characteristics of the surrounding concrete. It can simply take into account the effect of boundary conditions when the effect of moment loading in the anchoring area leads to a reduction in the resistance of (and to increasing losses in) the anchoring area. In addition, it is expected from the beginning of the development that the solution of the analytical relations will be automated, thus the development of a special software tool for anchoring area design is also being conducted.

Acknowledgment The presented results were obtained with the financial support of the Ministry of Industry and Trade project TIP FR-TI4/159 "Light structures-progressive construction made from advanced composite materials" and BUT internal grant agency project FAST-S-15-2899. "The use of advanced FRP materials in durable structures". This article was also supported by the Ministry of Education, Youth and Sport through Project CZ.1.07/2.3.00/30.0005-"Support for the creation of excellent interdisciplinary research teams at Brno University of Technology".

References

1. Al-Mayah A, Soudki K, Plumtree A (2001) Experimental and analytical investigation of a stainless steel anchorage for CFRP prestressing tendons. PCI J 46(2):88–100
2. Al-Mayah A, Soudki K, Plumtree A (2007) Novel anchor system for CFRP Rod: finite-element and mathematical models. J Compos Constr ASCE 11(5):469–476. doi:10.1061/(ASCE)1090-0268(2007)11:5(469)
3. Červenka V, Červenka J (2010) ATENA program documentation–ATENA 3D users manual. Červenka Consulting, Prague
4. Červenka V, Jendele L, Červenka J (2009) ATENA program documentation–ATENA theory. Červenka Consulting, Prague
5. EN 1992-1-1 (2006) Design of concrete structures. part 1-1: general rules and rules for buildings. ČNI, Prague
6. Dolan CV, Bakis CE, Nanni A (2001) Design recommendations for concrete structures prestressed with FRP tendons. FHWA Report, University of Wyoming, Pennsylvania State University, University of Missouri
7. Erki MA, Rizkalla SH (1993) FRP reinforcements for concrete structures. Concr Int 15(6):48–53
8. Erki MA, Rizkalla SH (1993) Anchorages for FRP reinforcement. Concr Int 15(6):54–59
9. Girgle F, Štěpánek P, Horák D, Daněk P, Kostiha V (2013) Newly developed anchoring element for prestressed FRP reinforcement–functionality and design, Proceedings of the FRPRCS 11–11th international symposium on fiber reinforced polymer for reinforced concrete structures. Universidade do Minho, Guimarães, Portugal, p 67. ISBN: 978-972-8692-84-1

10. Karbhari VM (1998) Use of composite materials in civil infrastructure in Japan. International Technology Research Institute, Word Technology Division, Baltimore
11. Kolář V, Němec I (1986) Study of a new model of subsoil (in Czech only; "Studie nového modelu podloží staveb"). ČSAV ACADEMIA, Prague
12. Li F, Zhao QL, Chen HS, Wang JQ, Duan HJ (2010) Prediction of tensile capacity based on cohesive zone model of bond anchorage for fiber-reinforced polymer tendon. Compos Struct 92:2400–2405. doi:10.1016/j.compstruct.2010.03.005
13. Nanni A, Bakis ChE, O'neil E, Dixon T (1996) Performance of FRP tendon-anchor systems for prestressed concrete structures. PCI J 41(1):34–44
14. Portnov GG, Bakis CE, Kulakov VL (2009) Assessment of transmission of the shear stress in potted anchors for composite rods–1. Part: sleeve of constant thickness. Mech Compos Mater 45(3):217–234. doi:10.1007/s11029-009-9087-4
15. Portnov GG, Bakis CE, Kulakov VL (2009) Assessment of transmission of the shear stress in potted anchors for composite rods–2. Part: sleeve of variable thickness. Mech Compos Mater 45(4):381–398. doi:10.1007/s11029-009-9099-0
16. Schmidt JW, Täljsten B, Bennitz A, Cowi AS (2009) FRP tendon anchorage in post-tensioned concrete structures. In: Alexander MG et al (eds) Concrete repair, rehabilitation and retrofitting II. Taylor & Francis Group, London
17. Soric Z, Kisicek T, Galic J (2010) Deflections of concrete beams reinforced with FRP bars. J Mater Struct 43:73–90. doi:10.1617/s11527-010-9600-1
18. Štěpánek P, Horák D, Prokeš J (2009) New prestressing system for FRP reinforcement in concrete structures, Proceedings of the 9th international symposium on fiber- reinforced polymer reinforcement for concrete structures, University of Adelaide, Sydney, Australia, ISBN: 978-0-9806755-0-4
19. Wu Z, Yang S, Zheng J, Hu X (2010) Analytical solution for the pull-out response of FRP rods embedded in steel tubes filled with cement grout. J Mater Struct 43:597–609. doi:10.1617/s11527-009-9515-x
20. Zhang BR, Benmokrane B, Chennouf A (2000) Prediction of tensile capacity of bond anchorages for FRP tendons. J Compos Constr 4(2):39–47. doi:10.1061/(ASCE)-0268(2000)4:2(39)
21. Zhang B, Benmokrane B (2002) Pullout bond properties of FRP tendons to grout. J Mater Civ Eng 14(5):399–408. doi:10.1061/(ASCE)0899-1561(2002)14:5(399)
22. Zhang B, Benmokrane B (2004) Design and evaluation of a new bond-type anchorage system for fiber reinforced polymer tendons. Can J Civ Eng 31:14–26. doi:10.1139/l03-062
23. *fib* Bulletin 72 (2014) Bond and anchorage of embedded reinforcement: background to the *fib* model code for concrete structures 2010, Lausanne, ISBN 978-2-88394-112-0